

This discussion paper is/has been under review for the journal Atmospheric Chemistry and Physics (ACP). Please refer to the corresponding final paper in ACP if available.

# Technical Note: Methods for interval constrained atmospheric inversion of methane

J. Tang<sup>1,2</sup> and Q. Zhuang<sup>1,2,3</sup>

<sup>1</sup>Department of Earth and Atmospheric Sciences, Purdue University, West Lafayette, Indiana, USA

<sup>2</sup>Purdue Climate Change Research Center, West Lafayette, Indiana, USA

<sup>3</sup>Department of Agronomy, Purdue University, West Lafayette, Indiana, USA

Received: 12 August 2010 – Accepted: 13 August 2010 – Published: 24 August 2010

Correspondence to: J. Tang (tang16@purdue.edu)

Published by Copernicus Publications on behalf of the European Geosciences Union.

19981

## Abstract

Three interval constrained methods, including the interval constrained Kalman smoother, the interval constrained maximum likelihood ensemble smoother and the interval constrained ensemble Kalman smoother are developed to conduct inversions of atmospheric trace gas methane (CH<sub>4</sub>). The negative values of fluxes in an unconstrained inversion are avoided in the constrained inversion. In a multi-year inversion experiment using pseudo observations derived from a forward transport simulation with known fluxes, the interval constrained fixed-lag Kalman smoother presents the best results, followed by the interval constrained fixed-lag ensemble Kalman smoother and the interval constrained maximum likelihood ensemble Kalman smoother. Consistent uncertainties are obtained for the posterior fluxes with these three methods. This study provides alternatives of the variable transform method to deal with interval constraints in atmospheric inversions.

## 1 Introduction

The atmospheric inversion modeling, often called the top-down approach, is an important way to quantify the magnitudes of various sources and sinks of trace gases (Enting, 2002). It proceeds by comparing the forward model simulations from an atmospheric transport model driven by sources and sinks from prior knowledge to the spatiotemporally discrete observations. The prior sources and sinks are then optimized to provide improved estimates through some optimization schemes, which are often reduced to minimizing a cost function that characterizes the differences between the forward model simulation and observations (e.g., Gurney et al., 2002).

Methods deduced from the Bayesian theorem (Tarantola, 2005), including the fixed-lag Kalman smoother (KS) (Hartley and Prinn, 1993; Bruhwiler et al., 2005), fixed-lag ensemble Kalman smoother (EnKS) (Peters et al., 2005) and fixed-lag maximum likelihood ensemble filter (Zupanski et al., 2007), have been widely used to invert the

19982

various trace gas fluxes. When used properly, those methods give reasonable posterior inferences conditioned on the available observations. However, in applying these methods to do inversions, sometimes the inverted results are of some physically inaccessible values. Therefore, these methods should be improved to impose proper

constraints, for instance, interval constraints as shown in this study, in addition to the constraints provided by observations.

To apply the interval constraints imposed over the state variables, the variable transform method can be applied efficiently, as was done in Tang and Zhuang (2010). However, the variable transform involved is non-linear, and is thus difficult to deal with using the KS, which is developed based on linear dynamics. Another problem with the variable transform method is the difficulty to interpret the posterior uncertainties, which are not defined in the same space of the inverted fluxes. In this note, we show the way to solve the problem using the interval constrained inversion methods. The proposed methods directly optimize the state variables in its original space, and the interval constraints are imposed either through a posterior correction or a direct constrained minimization. Three different methods developed are the interval constrained fixed-lag Kalman smoother (ICKS), interval constrained fixed-lag maximum likelihood ensemble smoother (ICMLES) and the interval constrained fixed-lag ensemble Kalman smoother (ICEnKS). These methods are evaluated with an inversion using pseudo observations of atmospheric CH<sub>4</sub> concentrations derived from a forward atmospheric transport of CH<sub>4</sub> with known fluxes.

## 2 Methods

### 2.1 The inversion problem and its lagged-form

$$z = \mathbf{H}s + \mathbf{v} \quad (1)$$

where  $z$  is the vector of observations,  $s$  is the vector of sinks and sources,  $\mathbf{H}$  is the sensitivity matrix that maps the flux  $s$  into measurement space, and  $\mathbf{v}$  is the uncertainty

19983

of the approximated observations  $\mathbf{H}s$  with respect to real observation  $z$ .

An inversion is to solve for  $s$  in Eq. (1) using the Bayes theorem, by assuming variables  $z$ ,  $s$  and  $\mathbf{v}$  as random variables with certain probability distributions (Tarantola, 2005).

In the lagged form, the forward equation Eq. (1) is

$$z_J = [\mathbf{H}_{J,J} \ \mathbf{H}_{J,J-1} \ \dots \ \mathbf{H}_{J,1}] [s_J^T \ s_{J-1}^T \ \dots \ s_1^T]^T + \mathbf{v} \quad (2)$$

$$= [\mathbf{H}_u \ \mathbf{H}_v] [s_u^T \ s_v^T]^T + \mathbf{v} \quad (3)$$

where  $s_u$  is defined by fluxes that are still being estimated, from time  $J$  back to time  $J-L+1$ , and  $s_v$  is defined by fluxes that are no longer updated, from time  $J-L$  back to time 1. The observation operators  $\mathbf{H}_u$  and  $\mathbf{H}_v$  are defined accordingly for  $s_u$  and  $s_v$ . Since  $s_v$  is no longer updated once it is obtained, we combine the term  $\mathbf{H}_v(s_v)$  into the measurement and denote the state variable by  $s$  to simplify the presentations hereinafter, unless explicitly stated otherwise.

### 2.2 The fixed-lag interval constrained Kalman smoother

By assuming normal distributions of the prior estimate and the measurements, the cost function solved by an interval constrained inversion is

$$\begin{aligned} \min J_1 &= (s - s^-)^T (\mathbf{Q}^-)^{-1} (s - s^-) \\ &\quad + [z - \mathbf{H}(s)]^T \mathbf{R}^{-1} [z - \mathbf{H}(s)] \\ &\quad | b_i < s_i < ub_i, \ i = 1, \dots, m \end{aligned} \quad (4)$$

where  $m$  is the length of the state vector  $s$ , and the superscript  $-$  denotes the prior estimate.

There are different ways to solve Eq. (4), e.g. the L-BFGS-B algorithm (Zhu et al., 1997). However, a two-stage strategy is used in this study to obtain the posterior estimate of the state variable and the covariance.

19984

At the first stage, Eq. (4) is solved as an unconstrained problem, which uses the Kalman update

$$\mathbf{s}^+ = \mathbf{s}^- + \mathbf{K}[\mathbf{z} - \mathbf{H}(\mathbf{s}^-)] \quad (5)$$

$$\mathbf{Q}^+ = (\mathbf{I} - \mathbf{KH})\mathbf{Q}^- \quad (6)$$

5 where the Kalman gain is

$$\mathbf{K} = \mathbf{Q}^-\mathbf{H}^T (\mathbf{R} + \mathbf{HQ}^-\mathbf{H}^T)^{-1} \quad (7)$$

10 Extension to including correlations between on-line (variables are still being updated) and off-line (variables that are no longer updated) state variables is straightforward (see Bruhwiler et al., 2005; Tang and Zhuang, 2010). However, for the specific problem in our study, the gain from accounting for such correlation is rather small, as we showed in Tang and Zhuang (2010).

At the second stage, the estimate from Kalman update at the first stage is updated to satisfy the interval constraints by minimizing the cost function

$$15 \min J_2 = (\mathbf{s} - \mathbf{s}^+)^T (\mathbf{Q}^+)^{-1} (\mathbf{s} - \mathbf{s}^+) \\ |b_i < s_i < ub_i, i = 1, \dots, m \quad (8)$$

Eq. (8) is solved iteratively with the active set method (Murty, 1988), just as documented in Tang and Zhuang (2010). When a set of active constraints are identified, the constraints are set to equality, such that

$$\mathbf{c}(\mathbf{s}^{++}) = \mathbf{0} \quad (9)$$

20 where the linear operator  $\mathbf{c}$  chooses the proper active constraints. Then a new solution is found using the Kalman update

$$\mathbf{s}^{++} = \mathbf{s}^+ - \mathbf{Q}^+\mathbf{c}^T (\mathbf{c}\mathbf{Q}^+\mathbf{c}^T)^{-1} (\mathbf{c}(\mathbf{s}^+)) \quad (10)$$

$$\mathbf{Q}^{++} = \mathbf{Q}^+ - \mathbf{Q}^+\mathbf{c}^T (\mathbf{c}\mathbf{Q}^+\mathbf{c}^T)^{-1} \mathbf{c}\mathbf{Q}^+ \quad (11)$$

19985

After the new solution is obtained, if there are still constraints being violated, the iteration is repeated until all interval constraints are satisfied. Zigzag may happen during iterations. Anti-cycling rules are sometimes needed to stop the iteration (Murty, 1988). However, we have not experienced such situation in this study.

### 5 2.3 The fixed-lag interval constrained maximum likelihood ensemble smoother

The maximum likelihood ensemble filter for unconstrained problem was proposed in Zupanski (2005), and documented in Zupanski et al. (2008). It uses a set of  $N+1$  ensemble simulations to approximate the covariance, and update the maximum likelihood estimation in the space spanned by the ensemble. In their formulation (Zupanski, 2005), a Hessian pre-conditioning is used to make the minimization problem well-posed. The posterior maximum likelihood estimation is obtained through the variable transform

$$\mathbf{s}^+ = \mathbf{s}^- + (\mathbf{Q}^-)^{1/2} (\mathbf{I} + \mathbf{C})^{-T/2} \xi \quad (12)$$

where the matrix  $\mathbf{C}$  is defined as

$$15 \quad \mathbf{C} = \mathbf{Z}^T \mathbf{Z} \quad (13)$$

$$\mathbf{Z}(\mathbf{s}) = [\mathbf{z}_1(\mathbf{s}), \mathbf{z}_2(\mathbf{s}), \dots, \mathbf{z}_N(\mathbf{s})] \quad (14)$$

$$\mathbf{z}_i(\mathbf{s}) = \mathbf{R}^{-1/2} [\mathbf{H}(\mathbf{s} + \mathbf{q}_i^-) - \mathbf{H}(\mathbf{s})] \quad (15)$$

where  $\mathbf{q}_i = \mathbf{s}_i - \mathbf{s}^-$ ,  $i=1, \dots, N$  are the prior perturbations, derived from the ensemble simulations with respect to the prior maximum likelihood estimator  $\mathbf{s}^-$ .

20 The gradient function used in minimization is

$$\mathbf{g}_\xi = (\mathbf{I} + \mathbf{C})^{-1} \xi - (\mathbf{I} + \mathbf{C})^{-1/2} \mathbf{Z}(\mathbf{s})^T \mathbf{R}^{-1/2} \\ \times \left\{ \mathbf{z} - \mathbf{H} \left[ \mathbf{s}^- + (\mathbf{Q}^-)^{1/2} \xi \right] \right\} \quad (16)$$

19986





A similar set up to that in Tang and Zhuang (2010) is used for the comparison experiment, so only necessary information is briefed here. Specifically, the sensitivity matrix is derived by running a group of tagged-CH<sub>4</sub> simulations using the GEOS-Chem model (Bey et al., 2001; Wang et al., 2004), driven by the GEOS-5 meteorology data at a resolution of 4° × 5°. Pseudo measurements are taken by sampling at 211 locations (excluding the towers) involved in the dataset of globalview-CH<sub>4</sub> 2009 (GLOBALVIEW-CH<sub>4</sub>, 2009). Sampling errors are simulated by using the relative residual error method (Palmer et al., 2003) derived by an optimized reference run against the globalview data. The prior fluxes are obtained by adding random perturbations to a set of known fluxes (11 seasonal fluxes and 7 yearly constant fluxes, see Tang and Zhuang, 2010), and are then used to obtain prior CH<sub>4</sub> concentrations at those sampling locations. The inversion is assessed by comparing the inverted fluxes and CH<sub>4</sub> concentrations to the known fluxes and CH<sub>4</sub> concentrations from the reference run.

### 3 Results and discussion

The prior fluxes and sampled prior CH<sub>4</sub> concentrations are shown in Fig. 1. Linear regression indicates the prior fluxes are rather poor approximations to the true fluxes. This makes the inversion difficult to get posterior fluxes to agree well with the known truth, as we will show below.

We first showed the results from the unconstrained inversion (Fig. 2). A lag length of 6 is used in all the inversions. It was shown in Tang and Zhuang (2010) such a lag length is sufficient to give stable inversions. All methods showed good posterior CH<sub>4</sub> concentrations compared to the observed data. However, because of the over-posed set up of the problem, unrealistic negative values of fluxes are inferred due to some spurious correlations among the different fluxes. We also compared the inversion using the MLES formulation in Zupanski (2005). It was found that their formulation provides slightly better posterior CH<sub>4</sub> concentrations. This can be explained by the use of eigen value screening in our study, which actually implies a greater null space of the state

19991

variables than that using the formulation in Zupanski (2005). Inclusion of correlation among on-line and off-line state variables does not help to keep the inverted fluxes within their feasible ranges (result not shown). Therefore, constrained inversion methods should be applied. This was achieved by using the variable transform technique in Tang and Zhuang (2010). There, reasonable posterior fluxes were obtained, but the posterior uncertainty is difficult to interpret. Thus, inversion methods that directly impose the constraint in the space of state variables are useful.

With the interval constrained methods, all inverted fluxes are in their feasible ranges (Fig. 3 and Table 1). The statistics of the posterior CH<sub>4</sub> concentrations are similar to that from the unconstrained inversion for KS and EnKS. The ICMLLES did not provide better posterior CH<sub>4</sub> concentrations than other methods when compared to the observations. For the posterior fluxes, ICKS performed the best, followed by the ICEnKS and ICMLLES. The posterior for the wetland emissions from the northwestern region (defined by 45° N north, 180° W to 0° W) in a typical year inverted from the three different interval constrained methods is shown in Fig. 4. We found that the three methods showed consistent estimates. All three methods have allowed the flux to be negative in the presence of uncertainty in the low emission months. This is a problem for unconstrained inversions, but not an issue for interval constrained inversions.

In addition, we tested the impact of ensemble sizes on the two ensemble-based interval constrained approaches. For ICEnKS, increasing the ensemble size to 200 or decreasing the ensemble size to 50, both give inferior results to the one using an ensemble size of 100 (see Fig. 5, Table 2). Similar results are observed for the ICMLLES when the ensemble size is increased or decreased (see Fig. 6, Table 2). The reason is that the covariance matrix is mostly determined by half of the eigen values, which is around 50 for the lag length of 6. This implies a pair-wised ensemble would be of size 100 (for ICEnKS), and an unpair-wised ensemble would be around 50 (for ICMLLES). An over-sampled ensemble or a sub-sampled ensemble will degrade the results.



- Wang, J. S., Logan, J., McElroy, M., Duncan, B., Megretskaja, I., and Yantosca, R.: A 3-D model analysis of the slowdown and interannual variability in the methane growth rate from 1988 to 1997, *Global Biogeochem. Cy.*, 18, GB3011, doi:10.1029/2003GB002180, 2004. 19991
- 5 Zhu, C., Byrd, R. H., and Nocedal, J.: L-BFGS-B: Algorithm 778: L-BFGS-B, FORTRAN routines for large scale bound constrained optimization, *ACM T. Math. Software*, 23, 550–560, 1997. 19984, 19987
- Zupanski, D., Denning, A., Uliasz, M., Zupanski, M., Schuh, A. E., Rayner, P. J., Peters, W., and Corbin, K. D.: Carbon flux bias estimation employing Maximum likelihood ensemble filter, *J. Geophys. Res.*, 112, D17107, doi:10.1029/2006JD008371, 2007. 19982
- 10 Zupanski, M.: Maximum likelihood ensemble filter: theoretical aspects, *J. Atmos. Sci.*, 133, 1710–1726, 2005. 19986, 19991, 19992, 19999
- Zupanski, M., Navon, I. M., and Zupanski, D.: The maximum likelihood ensemble filter as a non-differentiable minimization algorithm, *Q. J. Roy. Meteor. Soc.*, 134, 1039–1050, 2008. 19986

19995

**Table 1.** Statistics of the interval constrained inversion experiments against the observations.

Methods	Flux RMSE	Flux $R^2$	Concentration RMSE	Concentration $R^2$
ICKS	3.14	0.60	6.95	0.99
ICMLES	4.05	0.46	20.0	0.91
ICEnKS	3.16	0.59	8.5	0.98

19996



**Table 2.** Statistics of the interval constrained inversion experiments against the observations with different ensemble sizes.

Methods	Flux RMSE	Flux $R^2$	Concentration RMSE	Concentration $R^2$
ICMLES-20	4.00	0.41	24.3	0.90
ICMLES-100	4.29	0.42	29.2	0.80
ICEnKS-50	3.17	0.58	9.4	0.98
ICEnKS-200	3.25	0.57	10.5	0.98

19997

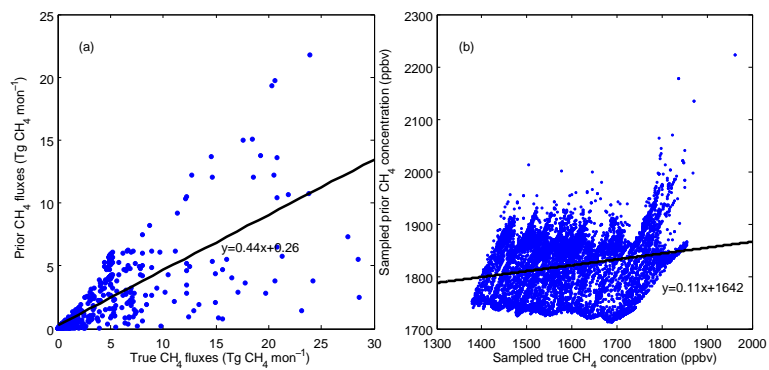


**Fig. 1.** (a) Prior fluxes; (b) prior CH<sub>4</sub> concentrations used in the inversion experiment.

19998

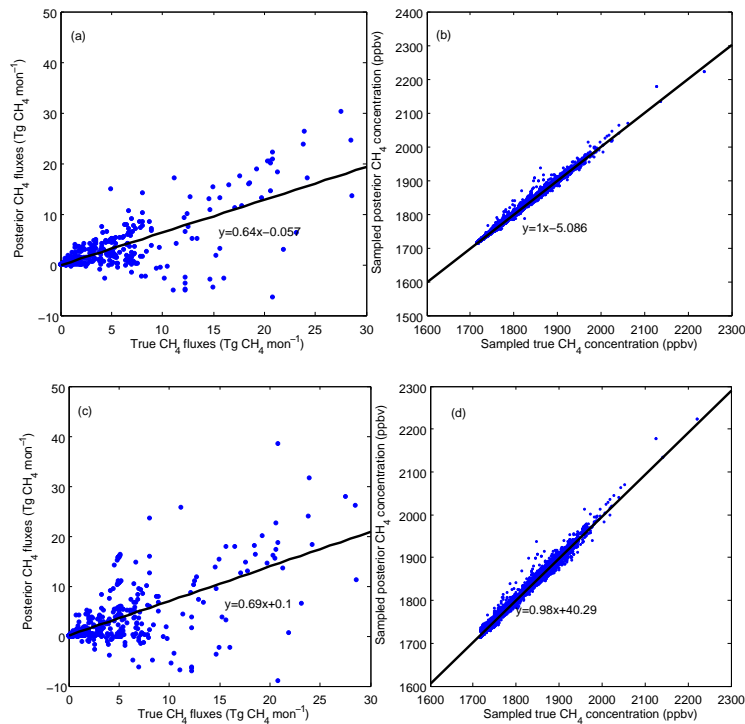


**Fig. 2.** (a) Posterior fluxes from unconstrained KS inversion; (b) posterior CH<sub>4</sub> concentrations from unconstrained KS inversion; (c) posterior fluxes from unconstrained MLES inversion, using Zupanski (2005)'s formulae; (d) posterior CH<sub>4</sub> concentrations from unconstrained inversion, using Zupanski (2005)'s formulae. An ensemble size of 50 is used for MLES inversion. The regressions are statistically significant with  $p < 0.0001$ .

19999

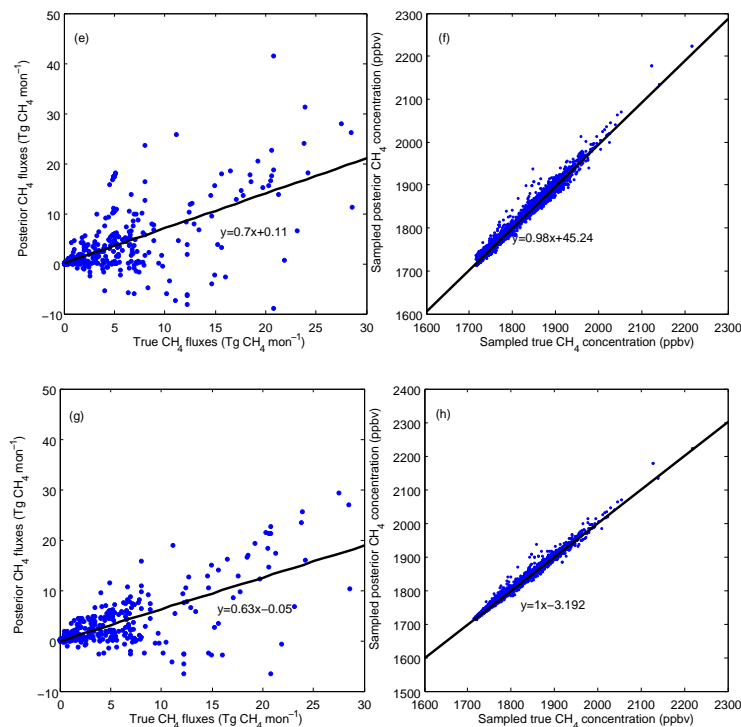


**Fig. 2.** (e) posterior fluxes from unconstrained MLES inversion, using formulae in this study; (f) posterior CH<sub>4</sub> concentrations from MLES inversion, using formulae in this study; (g) posterior fluxes from unconstrained EnKS inversion; (h) posterior CH<sub>4</sub> concentrations from EnKS inversion. A ensemble size of 50 is used for MLES inversion, and an ensemble size of 100 is used for EnKS inversion. The regressions are statistically significant with  $p < 0.0001$ .

20000

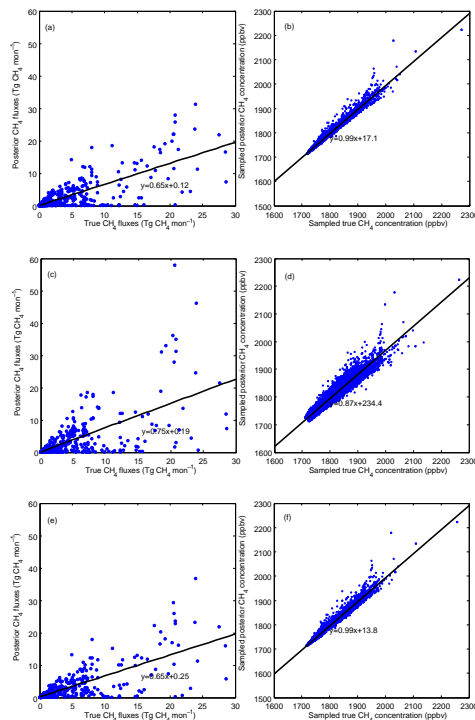


**Fig. 3.** (a) Posterior fluxes from ICKS inversion; (b) posterior CH<sub>4</sub> concentrations from ICKS inversion; (c) posterior fluxes from ICMLES inversion; (d) posterior CH<sub>4</sub> concentrations from ICMLES inversion; (e) posterior fluxes from ICEnKS inversion; (f) posterior CH<sub>4</sub> concentrations from ICEnKS inversion. A ensemble size of 50 is used for ICMLES inversion, and an ensemble size of 100 is used for ICEnKS inversion. The regressions are statistically significant with  $p < 0.0001$ .

20001

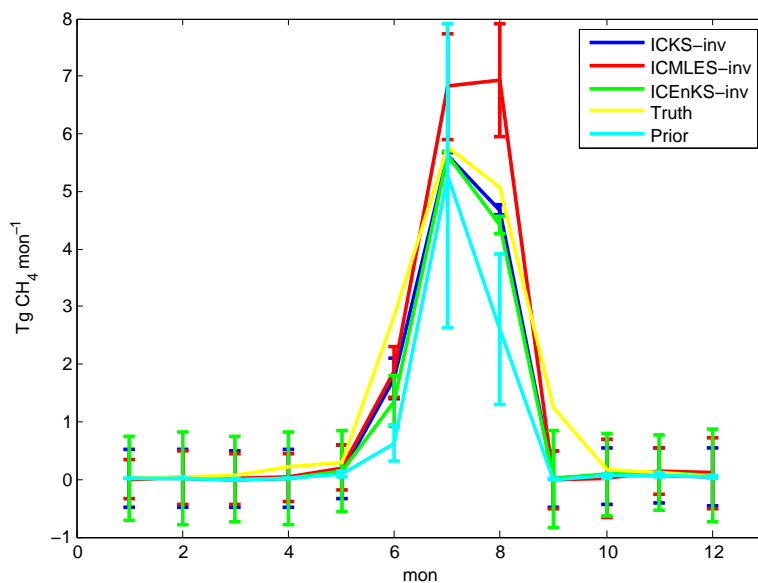


**Fig. 4.** Comparison of posterior inference from different interval constrained inversions for the wetland emissions from the north western region defined by 45° N north, 180° W to 0°.

20002

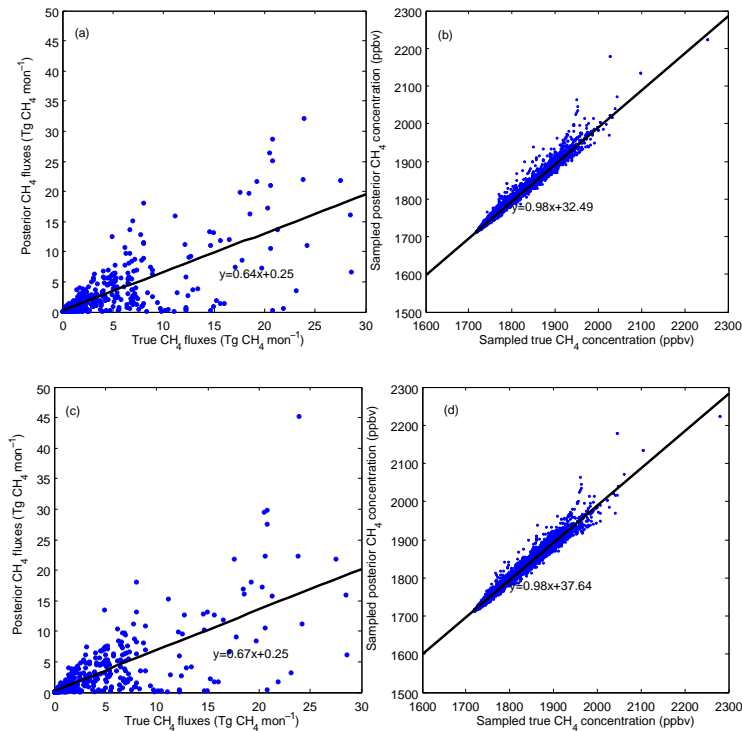


**Fig. 5.** (a) Posterior fluxes from ICEnKS inversion, with ensemble size equals to 50; (b) posterior CH<sub>4</sub> concentrations from ICEnKS inversion, with ensemble size equals to 50; (c) posterior fluxes from ICEnKS inversion, with ensemble size equals to 200; (d) posterior CH<sub>4</sub> concentrations from ICEnKS inversion, with ensemble size equals to 200. The regressions are statistically significant with  $p < 0.0001$ .

20003

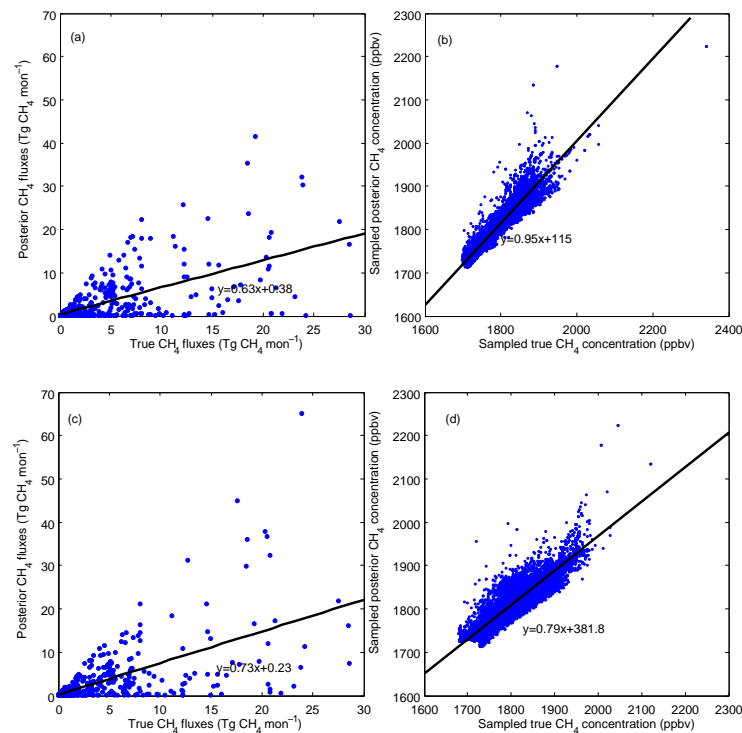


**Fig. 6.** (a) Posterior fluxes from ICMLES inversion, with ensemble size equals to 20; (b) posterior CH<sub>4</sub> concentrations from ICMLES inversion, with ensemble size equals to 20; (c) posterior fluxes from ICMLES inversion, with ensemble size equals to 100; (d) posterior CH<sub>4</sub> concentrations from ICMLES inversion, with ensemble size equals to 100. The regressions are statistically significant with  $p < 0.0001$ .

20004